State-of-Charge Estimation for Batteries Based on the Nonlinear Double-Capacitor Model and Extended Kalman Filter

Mason Proctor*, Ning Tian†, and Huazhen Fang‡
Department of Mechanical Engineering, University of Kansas
Lawrence, KS, USA
Email: *masonjproc@ku.edu, †ning.tian@ku.edu, ‡fang@ku.edu

***Abstract*—State-of-charge (SOC) estimation plays a foundational role in advanced battery management systems (BMS), having attracted much attention in the past decade. It is widely acknowledged that the accuracy of SOC estimation largely depends on the accuracy of the selected model. In this work, we contribute a new SOC estimation method based on the nonlinear double-capacitor (NDC) model, a novel equivalent circuit model distinctly capable of simulating the charge diffusion inside an electrode of a battery and capturing the battery's nonlinear voltage behavior simultaneously. With improved predictive accuracy, the NDC model provides a new opportunity for enabling more accurate SOC estimation. With this motivation, this paper exploits the well-known extended Kalman filter (EKF) to perform SOC estimation based on the NDC model. The EKF is desirable here as it leads to efficient computation, straightforward implementation, and good convergence in its application to the NDC model, which is low-dimensional and governed by linear dynamics along with nonlinear output. The proposed SOC estimation method is validated through simulations and experimental data under various conditions, showing significant accuracy as well as robustness to different levels of initialization error and noises.**

***Index Terms*—State-of-charge, nonlinear double-capacitor, battery management systems, extended Kalman filter.**

I. Introduction

As the world has become increasingly dependent on electronic devices, from small scale portable electronics like cell phones and laptops, to larger scale systems such as electric vehicles and grid energy storage, rechargeable batteries have become a major focus of many research and development efforts. Battery energy storage is a technology crucial for the worldwide shift to renewable energy, as it will support and complement the existing power grid [1], [2] to accommodate the influx of electric vehicles, solar panels, and wind turbines. The successful implementation of rechargeable battery-based energy storage systems requires a battery management system (BMS) to monitor and control the battery operation [3]. Among its various functions, arguably the most important is the state-of-charge estimation, which has attracted considerable research in the past years but still remains an open challenge due to the incessant demand for better accuracy.

The SOC of a battery is defined as the ratio of available capacity to the total capacity and is commonly shown as a percentage value on devices such as cell phones and laptops. To the everyday user it may seem to be a trivial calculation, but unfortunately this is not the case and some sort of algorithm is necessary to infer the SOC from current, voltage, and temperature measurements. An accurate SOC knowledge is required in advanced battery management systems, such as those in electric vehicles, for several purposes. In order to avoid overcharge and overdischarge of the batteries [4], which can result in fire or explosion [5], the user must accurately know the cell charge level. The SOC also acts as a reference to cell balancing strategies, power calculations, and energy calculations [6]. Poor charging and discharging strategies can reduce the lifetime of a battery, therefore knowing the SOC can help avoid these problems. An overview of various SOC estimation techniques is discussed below.

SOC estimation methods can be separated into two groups: traditional model-free methods and recent but increasingly popular model-based and data-based methods. Traditional methods do not make use of battery models and rely on measurements or straightforward calculations. One such ubiquitous method is coulomb counting, where the SOC of a cell is tracked by the integration of current over time. This method is highly reliant on an accurate initial current reading and is subject to drift, making it inadequate for advanced battery applications [3]. Another traditional technique is voltage translation, in which an open-circuit-voltage (OCV) measurement is taken and the SOC is found from an SOC-OCV lookup table or curve that was determined offline. This method is cumbersome and impractical due to the rest period needed to measure OCV [7].

New methods to estimate SOC make use of either advanced data-driven or physics-based models. Most recently, machine learning methods such as artificial neural networks [8] and support vector machines [9] have been proposed for estimating SOC, where a data-driven predictive model is built by training the battery data sets, but this must be done offline and takes time. In the literature, there are two predominant model-based SOC estimation methods for batteries – electrochemical models or equivalent circuit models (ECMs). Electrochemical models characterize the ion transport within the battery, therefore requiring a set of partial differential equations (PDEs) to be solved [10], [11], which is too computationally expensive to be

useful in real-time BMS SOC monitoring often implemented on an embedded processing chip [12]. ECMs, however, offer a computationally appealing alternative to electrochemical model-based SOC estimation. ECMs simulate the current-voltage behavior of a battery by modeling the battery as an electric circuit with well-known components, such as voltage sources, resistors, and capacitors. ECMs are much simpler and more computationally efficient than electrochemical models, which make ECMs great candidates for use in advanced BMSs that require real-time estimation of various battery states, especially SOC [13].

Within the model-based SOC estimation field, there exist nonlinear observers and stochastic estimators. Among the nonlinear SOC observers are Luenberger observers, sliding-mode observers and robust nonlinear observers [10], which view the battery model as a deterministic system. On the other hand, stochastic estimators possess the ability to suppress the noise that naturally occurs within and affects a dynamic system [7]. The Kalman filter, a recursive and probabilistic technique, is the most notable of this type, which has been used to address a broad range of stochastic estimation problems [14]. The extended Kalman filter (EKF) is a nonlinear extension of the standard Kalman filter for nonlinear systems and has become an increasingly important approach for SOC estimation, mainly due to its amenability to design. Another advantage of the EKF is its competitiveness in terms of computational cost and convergence when applied to models with low order—even though it has cubic computational complexity, the actual computation will still be low for low-dimensional models such as most ECMs for batteries [15].

To meet the growing need for accurate SOC knowledge, this paper exploits a novel battery model, i.e., the nonlinear double-capacitor (NDC) model, and the EKF to develop a new SOC estimation approach. As shown in Fig. 1, the NDC model was recently proposed in [16] and shows better predictive accuracy than other popular ECMs, primarily ascribed to its capability of simultaneously simulating the diffusion of charge within an electrode and capturing the nonlinear voltage behavior. This implies a new opportunity for enabling more precise SOC estimation using this model. Here, the EKF is an appealing choice to perform the estimation for two reasons. First, the NDC model has only three states, thus allowing for efficient computation involved in executing the EKF. Second, the nonlinearity of the NDC model lies only in the measurement process, which makes the linearization easier while simplifying the implementation of the EKF. This proposed approach is then evaluated extensively via simulation and experiments.

This paper is organized as follows. Section II is an overview of the NDC model as formulated in [16]. Section III describes the EKF estimation approach used in this work. Section IV provides an extensive validation of the proposed SOC estimation method, including simulation results and experimental results. Section V concludes the paper and includes a brief discussion of future work directions.

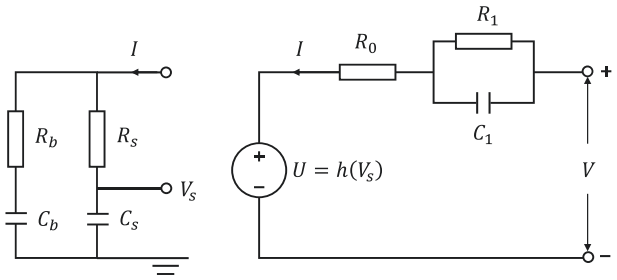

Fig. 1: The nonlinear double-capacitor model.

II. Nonlinear Double-Capacitor Model

In this section, the NDC model is introduced and an overview of the motivation for its development and the mathematical equations characterizing its behavior are presented.

The NDC model, an extension of the double-capacitor model [17], [18], was developed to enhance the competence of ECMs in better capturing a battery's electric behavior. This model makes use of two parallel resistor-capacitor (RC) circuits to characterize the charge diffusion within an electrode of a battery. Each R-C branch represents a region of the electrode. Specifically, the R_b-C_b circuit represents the bulk portion of the electrode, and the R_s-C_s circuit represents the surface region of the electrode which is in contact with the electrolyte. In Fig. 1, V_s is the voltage across C_s, and V_b (not shown) is the voltage across C_b. V_b and V_s are set to be between 0 and 1 V. Based on such an analogy, this circuit structure can offer an emulation of the charge diffusion process inside an electrode, which is the most important part of a battery's dynamics. In addition, a battery's voltage behavior is nonlinear, mainly due to the nonlinear SOC-OCV relationship. The NDC model thus includes a nonlinear mapping of V_s, i.e., $U = h(V_s)$. It is further complemented with the internal resistor R_0 and R_1-C_1 circuit.

The dynamics of the NDC model, in state-space form, is shown as follows.

$$\begin{bmatrix} \dot{V}_b(t) \\ \dot{V}_s(t) \\ \dot{V}_1(t) \end{bmatrix} = A \begin{bmatrix} V_b(t) \\ V_s(t) \\ V_1(t) \end{bmatrix} + BI(t) \tag{1a}$$

$$V(t) = h(V_s(t)) - V_1(t) + R_0 I(t) \tag{1b}$$

where

$$A = \begin{bmatrix} \frac{-1}{C_b(R_b+R_s)} & \frac{1}{C_b(R_b+R_s)} & 0 \\ \frac{1}{C_s(R_b+R_s)} & \frac{-1}{C_s(R_b+R_s)} & 0 \\ 0 & 0 & \frac{-1}{R_1 C_1} \end{bmatrix}, B = \begin{bmatrix} \frac{R_s}{C_b(R_b+R_s)} \\ \frac{R_b}{C_s(R_b+R_s)} \\ \frac{-1}{C_1} \end{bmatrix}$$

In the nonlinear measurement equation, the $h(V_s)$ term can be parameterized as a fifth-order polynomial and is written as

$$h(V_s) = \alpha_0 + \alpha_1 V_s + \alpha_2 V_s^2 + \alpha_3 V_s^3 + \alpha_4 V_s^4 + \alpha_5 V_s^5$$

Here, SOC is dependent on the states as follows:

$$\text{SOC} = \frac{Q_a}{Q_t} = \frac{C_b V_b + C_s V_s}{C_b + C_s} \times 100\%$$

where Q_a is the available capacity and Q_t is the total capacity. This relation suggests that SOC estimation is a state estimation problem. Furthermore, the internal resistance R_0 is dependent on SOC and is described by

$$R_0 = \gamma_1 + \gamma_2 e^{-\gamma_3 \mathrm{SOC}} + \gamma_4 e^{-\gamma_5(1-\mathrm{SOC})}$$

With its unique circuit structure, the NDC model can more accurately predict the OCV and the charge diffusion in the electrodes, making it advantageous for SOC estimation.

III. State-of-Charge Estimation Using EKF

A. Problem Formulation

We focus on the problem of estimating the SOC of rechargeable battery cells in real-time based on the NDC model using current and voltage measurements. To accomplish this goal, we begin from the continuous-time model (1). The discrete state-space model takes the form

$$\begin{aligned} x_{k+1} &= Fx_k + Gu_k + w_k \\ y_k &= \bar{h}(x_k, u_k) + v_k \end{aligned}$$

where $F = e^{AT}, G = (\int_0^T e^{A\tau} d\tau)B$, x_k is the state at time k, u_k is the input current at time k, y_k is the voltage measurement at time k, and $\bar{h}(x_k, u_k)$ is the nonlinear transformation describing the terminal voltage measurement as a function of the state and input at time k. Here, $\{w_k\}$ is added to represent the process noise and assumed to be a white Gaussian noise sequence with the distribution $w_k \sim \mathcal{N}(0, Q)$, and $\{v_k\}$ is added to capture the measurement noise which is also considered a white Gaussian noise sequence with $v_k \sim \mathcal{N}(0, R)$.

Now, we have a model ready to track the three state variables, V_b, V_s, and V_1, at each time instant from which SOC can be inferred directly. The low dimensionality and nonlinearity of this model invites the use of the EKF. It is straightforward to apply the EKF to a system of only three dimensions, and because the primary difficulty in solving this problem lies in the nonlinear measurement equation, the linearization done by the EKF is an efficient choice and allows us to overcome this obstacle.

B. EKF Algorithm Implementation

In this section, the implementation of the EKF will be presented. The EKF is performed in three steps: *initialization*, *state prediction (time update)*, and *state update (measurement update)*. The state prediction and state update steps are computed recursively at each time instant. Before this recursion takes place, we must carefully consider the initialization step. Not only are we considering the initial values of the state estimate statistics, but we must also select appropriate noise covariance matrices. The selection of these covariance matrices, Q and R, is crucial to the estimation performance and convergence of the EKF, and an incorrect choice may result in the SOC estimate diverging greatly from the truth. We select Q based on our confidence in the model, and we select R based on the measurement uncertainty.

TABLE I: NDC model parameters.

C_b	C_s	R_b	R_s	R_1	C_1
10037 $[F]$	973 $[F]$	0.019 $[\Omega]$	0 $[\Omega]$	0.02 $[\Omega]$	3250 $[F]$

TABLE II: Simulation test design.

Test #	Initialization Error	Process Noise Level	Measurement Noise Level
1	5%	$10^{-5} I_3$	0.05^2
2	5%	$10^{-5} I_3$	2.5×10^{-6}
3	5%	$10^{-8} I_3$	0.05^2
4	5%	$10^{-8} I_3$	2.5×10^{-6}
5	20%	$10^{-5} I_3$	0.05^2
6	20%	$10^{-5} I_3$	2.5×10^{-6}
7	20%	$10^{-8} I_3$	0.05^2
8	20%	$10^{-8} I_3$	2.5×10^{-6}

We begin by initializing the state estimate mean and state estimate covariance:

$$\begin{aligned} \hat{x}_0 &= \mathrm{E}[x_0] \\ P_0^x &= \mathrm{E}[(x_0 - \hat{x}_0)(x_0 - \hat{x}_0)^T] \end{aligned}$$

The state estimate is represented as a random vector whose probability distribution is described by $x_k | Y_{k-1} \sim \mathcal{N}(\hat{x}_{k|k-1}, P^x_{k|k-1})$, where Y_{k-1} is the set of measurements up to time $k-1$, $\hat{x}_{k|k-1}$ is the estimate of x_k given Y_{k-1}, and $P^x_{k|k-1}$ is the covariance of the state estimate at time k given Y_{k-1}. These statistics, i.e., the mean and covariance of the distribution, are then propagated through the time update and measurement update steps as shown below.

State Prediction (Time Update)

$$\begin{aligned} \hat{x}_{k|k-1} &= F\hat{x}_{k-1|k-1} + Gu_{k-1} \\ P^x_{k|k-1} &= FP^x_{k-1|k-1}F^T + Q \end{aligned}$$

When the new measurement y_k is made available, the filter can update its knowledge of the state x_k at time k by $x_k | Y_k \sim \mathcal{N}(\hat{x}_{k|k}, P^x_{k|k})$.

State Update (Measurement Update)

$$\begin{aligned} \hat{x}_{k|k} &= \hat{x}_{k|k-1} + P^x_{k|k-1}\bar{H}_k^T(\bar{H}_k P^x_{k|k-1}\bar{H}_k^T + R)^{-1} \\ &\qquad \times [y_k - \bar{h}(\hat{x}_{k|k-1})] \\ P^x_{k|k} &= P^x_{k|k-1} - P^x_{k|k-1}\bar{H}_k^T(\bar{H}_k P^x_{k|k-1}\bar{H}_k^T + R)^{-1}\bar{H}_k P^x_{k|k-1} \end{aligned}$$

In the above equations, $\bar{H}_k$ is the Jacobian matrix, defined as

$$\bar{H}_k = \left.\frac{\partial \bar{h}}{\partial x}\right|_{\hat{x}_{k|k-1}} = \begin{bmatrix} (-\gamma_2\gamma_3 e^{-\gamma_3 \hat{\mathrm{SOC}}} + \gamma_4\gamma_5 e^{-\gamma_5(1-\hat{\mathrm{SOC}})}) I(k) \frac{C_b}{Q_t} \\ \frac{\partial h(\hat{V}_s)}{\partial x} + (-\gamma_2\gamma_3 e^{-\gamma_3 \hat{\mathrm{SOC}}} + \gamma_4\gamma_5 e^{-\gamma_5(1-\hat{\mathrm{SOC}})}) I(k) \frac{C_s}{Q_t} \\ -1 \end{bmatrix}^T$$

TABLE III: SOC estimation error: Simulation.

Test #	1	2	3	4	5	6	7	8
Error (%)	3.6	7.6	0.35	0.16	4.9	7.8	0.47	0.29

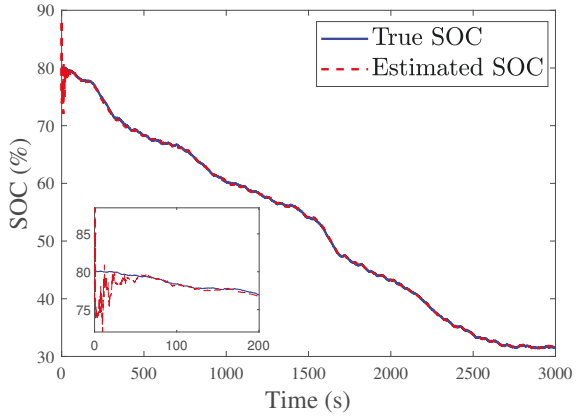

Fig. 2: SOC estimation for simulation #4 in Table II: Low initialization error with low process noise and low measurement noise.

where

$$\hat{\text{SOC}} = \frac{C_b\hat{V}_b + C_s\hat{V}_s}{C_b + C_s}$$

$$\frac{\partial h(\hat{V}_s)}{\partial x} = \alpha_1 + 2\alpha_2\hat{V}_s + 3\alpha_3\hat{V}_s^2 + 4\alpha_4\hat{V}_s^3 + 5\alpha_5\hat{V}_s^4$$

The EKF provides an ideal choice for SOC estimation based on the NDC model. First, whichever filter we use will be implemented in an embedded system with limited computational resources. The EKF is a good choice for this application to the NDC model, as the model is three-dimensional and the EKF is competitive in computational complexity and convergence for low-dimensional systems [15]. Another reason for choosing the EKF is the ease of tuning relative to other filters. For example, in the unscented Kalman Filter (UKF) one must select appropriate values for α, β, and γ parameters as well as the process noise covariance matrix Q and measurement noise covariance matrix R, whereas with the EKF we only have to tune the Q and R matrices. The measurement noise can be found from the root-mean-squared (RMS) noise values specified by the measurement device, so we are mostly concerned with the selection of Q, which characterizes our confidence in the process model and does not represent any real physical process. Applying the EKF may be tedious for some models due to the computation of the Jacobian matrices. However, for the NDC model only the measurement equation is nonlinear and the computation of the Jacobian is straightforward. Lastly, the EKF has been extensively used for various SOC estimation applications in the literature [19]–[23], proving its effectiveness. Other estimation methods may be used for this application, which will be a part of future exploration.

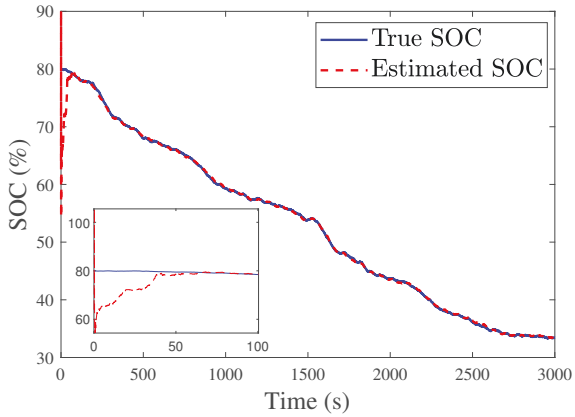

Fig. 3: SOC estimation for simulation #8 in Table II: High initialization error with low process noise and low measurement noise.

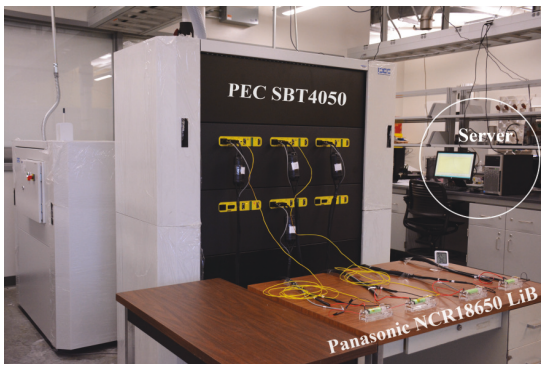

Fig. 4: PEC SBT4050 battery cycler test bench set-up.

IV. Method Validation

In this section, we present simulation and experimental results to validate the proposed SOC estimation method. Using simulations, we will assess the robustness of the method against SOC initialization error and noises at different levels. Then, we will further appraise the method using experimental data.

A. Numerical Simulation

The NDC model was simulated using the parameters shown in Table I, which were identified for a Panasonic NCR18650B lithium-ion battery cell in [16]. The fifth-order polynomial $h(\cdot)$ takes the form as follows:

$$h(V_s) = 3.2 + 2.59 \cdot V_s - 9.003 \cdot V_s^2 + 18.87 \cdot V_s^3 - 17.82 \cdot V_s^4 + 6.325 \cdot V_s^5$$

The internal resistance, as a function of SOC, is described by

$$R_0 = 0.0531 + 0.1077e^{-3.807\cdot\text{SOC}} + 0.0533e^{-7.613(1-\text{SOC})}$$

Now that we have a parameterized NDC model, we can proceed to validate the estimation method. To evaluate the robustness of the method against varying initialization errors and noise levels, we designed and performed numerous simulations based on combinations of three factors: the initialization

TABLE IV: Experiment test design.

Test #	1	2	3	4
Initialization Error (%)	5	20	50	75

TABLE V: SOC estimation error: Experimental data.

Test #	1	2	3	4
Error (%)	1.38	1.42	1.48	1.56

error, Q, and R, to control for each robustness metric. Each factor can assume one of two modes. Here, we let the SOC initialization error take the values 5% or 20%, $Q = 10^{-8}I_3$ or $Q = 10^{-5}I_3$ (where I_3 denotes the identity matrix of dimension 3), and $R = 2.5 \times 10^{-6}$ or $R = 0.05^2$. Table II outlines the eight cases considered in the simulation setting. For this method to be applicable in general practice, it needs to be robust to SOC initialization error because the BMS may not always know the initial SOC of the cell in question, and it needs to be able to adequately track the SOC in the case of large process and measurement noise levels.

Based on the simulation results, we find that the proposed method has considerable robustness to different levels of initialization errors and noise levels. This robustness will make the method advantageous in real-world applications. The EKF is able to accurately track the SOC of the battery and converge quickly, even under large noise and initialization error conditions, with an average SOC estimation error of 3.1% across all simulations, with a maximum error of 7.8%. The results of the simulations are summarized in Table III, and two cases are plotted in Figs. 2 and 3 showing accurate and convergent SOC tracking under different initialization errors.

B. Experimental Validation

The battery cycling experiments presented in this paper were conducted on a PEC SBT4050 battery tester, shown in Fig. 4. The battery tester is capable of up to 40 V and 50 A charging/discharging and can be programmed for specific test regimes. The server is where specific testing regimes can be formulated offline and the data were collected using LifeTest software. Experiments were performed on a Panasonic NCR18650B lithium-ion battery cell, with a nominal voltage of 3.7 V and a capacity of 3.4 Ah.

For the experimental validation, we analyze the estimation accuracy under different initialization errors. Experimental data, shown in Fig. 5, were used to verify the proposed SOC estimation algorithm. These experiments were conducted under variable currents normalized from Urban Dynamometer Drive Schedule (UDDS) profile [24] and scaled to a discharging range of 0–3 A. Similar to the simulation testing design, the experimental test cases can be seen in Table IV. In the experimental setting, SOC obtained by coulomb counting is used as a reference for comparison, which is used as a benchmark to evaluate the estimation by the EKF [25]. Using the experimental data, the EKF was able to track the SOC of the battery very well, with an average SOC error of around 1.46%, as reported in Table V. Fig. 6 shows accurate and convergent SOC tracking under high initialization error.

V. Conclusions and Future Work

SOC estimation is a fundamental problem in BMS applications. In this work, we explored SOC estimation using the NDC model, a novel ECM for rechargeable batteries, and developed an estimation algorithm based on an EKF. The proposed method showed excellent SOC estimation accuracy and convergence under various noise levels and initialization error conditions in simulations as well as with experimental data. Our future work will extend the results to SOC estimation with temperature awareness by way of a more sophisticated version of the NDC model.

References

[1] A. Castillo and D. F. Gayme, "Grid-scale energy storage applications in renewable energy integration: A survey," *Energy Conversion and Management*, vol. 87, pp. 885 – 894, 2014.

[2] B. Dunn, H. Kamath, and J.-M. Tarascon, "Electrical energy storage for the grid: A battery of choices," *Science*, vol. 334, no. 6058, pp. 928–935, 2011.

[3] V. Pop, H. J. Bergveld, D. Danilov, P. P. Regtien, and P. H. Notten, "State-of-the-art of battery state-of-charge determination," *Battery Management Systems: Accurate State-of-Charge Indication for Battery-Powered Applications*, pp. 11–45, 2008.

[4] M. Hannan, M. Lipu, A. Hussain, and A. Mohamed, "A review of lithium-ion battery state of charge estimation and management system in electric vehicle applications: Challenges and recommendations," *Renewable and Sustainable Energy Reviews*, vol. 78, pp. 834 – 854, 2017.

[5] Q. Wang, P. Ping, X. Zhao, G. Chu, J. Sun, and C. Chen, "Thermal runaway caused fire and explosion of lithium ion battery," *Journal of Power Sources*, vol. 208, pp. 210 – 224, 2012.

[6] G. Plett, *Battery Management Systems, Volume II: Equivalent-Circuit Methods*, ser. Artech House Power Engineering Series. Artech House, 2015.

[7] Y. Wang, H. Fang, L. Zhou, and T. Wada, "Revisiting the state-of-charge estimation for lithium-ion batteries: A methodical investigation of the extended kalman filter approach," *IEEE Control Systems Magazine*, vol. 37, no. 4, pp. 73–96, Aug 2017.

[8] M. Charkhgard and M. Farrokhi, "State-of-charge estimation for lithium-ion batteries using neural networks and EKF," *IEEE Transactions on Industrial Electronics*, vol. 57, no. 12, pp. 4178–4187, 2010.

[9] J. Hu, J. Hu, H. Lin, X. Li, C. Jiang, X. Qiu, and W. Li, "State-of-charge estimation for battery management system using optimized support vector machine for regression," *Journal of Power Sources*, vol. 269, pp. 682–693, 2014.

[10] S. Dey, B. Ayalew, and P. Pisu, "Nonlinear robust observers for state-of-charge estimation of lithium-ion cells based on a reduced electrochemical model," *IEEE Transactions on Control Systems Technology*, vol. 23, no. 5, pp. 1935–1942, 2015.

[11] R. Klein, N. A. Chaturvedi, J. Christensen, J. Ahmed, R. Findeisen, and A. Kojic, "Electrochemical model based observer design for a lithium-ion battery," *IEEE Transactions on Control Systems Technology*, vol. 21, no. 2, pp. 289–301, 2013.

[12] L. Zhang, B. Tiwana, Z. Qian, Z. Wang, R. P. Dick, Z. M. Mao, and L. Yang, "Accurate online power estimation and automatic battery behavior based power model generation for smartphones," in *Proceedings of the Eighth IEEE/ACM/IFIP International Conference on Hardware/Software Codesign and System Synthesis*, ser. CODES/ISSS '10. New York, NY, USA: ACM, 2010, pp. 105–114.

[13] G. Plett, *Battery Management Systems, Volume I: Battery Modeling*, ser. Artech House Power Engineering Series. Artech House, 2015.

[14] B. D. Anderson and J. B. Moore, *Optimal filtering*. Courier Corporation, 2012.

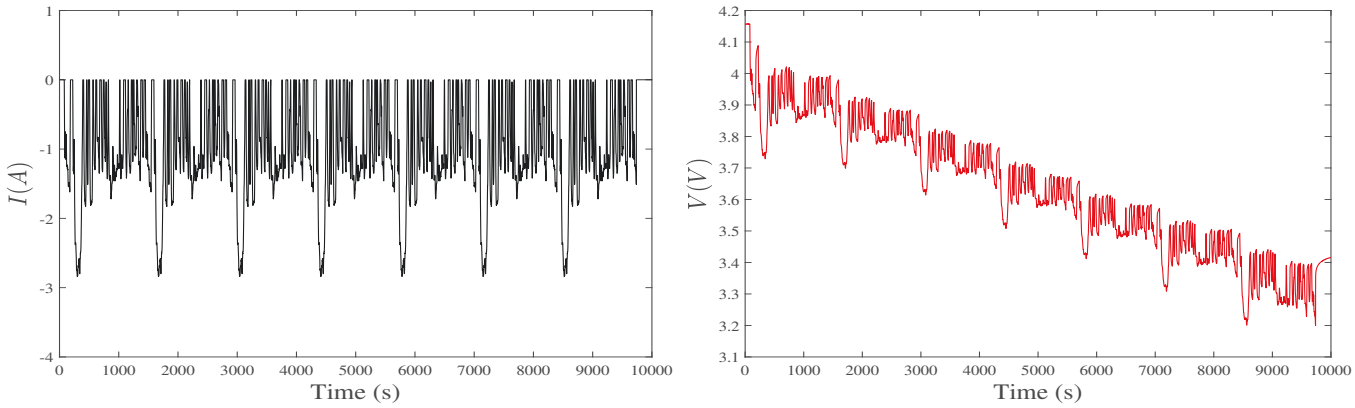

(a) (b)

Fig. 5: (a) UDDS-based current profile; (b) measured terminal voltage.

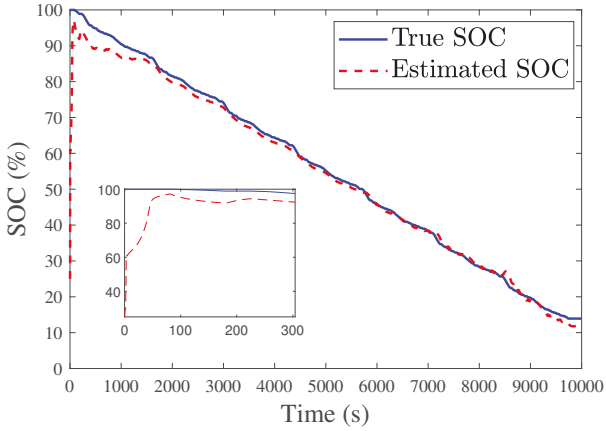

Fig. 6: SOC estimation based on the experimental data using the setting #4 in Table IV.

[15] H. Fang, N. Tian, Y. Wang, M. Zhou, and M. A. Haile, "Nonlinear Bayesian estimation: from Kalman filtering to a broader horizon," *IEEE/CAA Journal of Automatica Sinica*, vol. 5, no. 2, pp. 401–417, 2018.

[16] N. Tian, H. Fang, J. Chen, and Y. Wang, "Nonlinear double-capacitor model for rechargeable batteries: Modeling, identification and validation," arXiv preprint arXiv:1906.04150, 2019.

[17] V. Johnson, A. Pesaran, and T. Sack, "Temperature-dependent battery models for high-power lithium-ion batteries," in *17th Annual Electric Vehicle Symposium*, Jan. 2001.

[18] V. Johnson, "Battery performance models in ADVISOR," *Journal of Power Sources*, vol. 110, no. 2, pp. 321–329, 2002.

[19] Z. Chen, Y. Fu, and C. C. Mi, "State of charge estimation of lithium-ion batteries in electric drive vehicles using extended Kalman filtering," *IEEE Transactions on Vehicular Technology*, vol. 62, no. 3, pp. 1020–1030, March 2013.

[20] W. Junping, G. Jingang, and D. Lei, "An adaptive Kalman filtering based State of Charge combined estimator for electric vehicle battery pack," *Energy Conversion and Management*, vol. 50, no. 12, pp. 3182 – 3186, 2009.

[21] H. Fang, Y. Wang, Z. Sahinoglu, T. Wada, and S. Hara, "Adaptive estimation of state of charge for lithium-ion batteries," in *2013 American Control Conference*, June 2013, pp. 3485–3491.

[22] J. Han, D. Kim, and M. Sunwoo, "State-of-charge estimation of lead-acid batteries using an adaptive extended Kalman filter," *Journal of Power Sources*, vol. 188, no. 2, pp. 606–612, 2009.

[23] S. Nejad, D. Gladwin, and D. Stone, "A systematic review of lumped-parameter equivalent circuit models for real-time estimation of lithium-ion battery states," *Journal of Power Sources*, vol. 316, pp. 183–196, 2016.

[24] The EPA Urban Dynamometer Driving Schedule (UDDS). [Online]. Available: https://www.epa.gov/sites/production/files/2015-10/uddscol.txt

[25] K. S. Ng, C.-S. Moo, Y.-P. Chen, and Y.-C. Hsieh, "Enhanced coulomb counting method for estimating state-of-charge and state-of-health of lithium-ion batteries," *Applied Energy*, vol. 86, no. 9, pp. 1506–1511, 2009.